Engineering Advanced Capsosomes: Maximizing the Number of Subcompartments, Cargo Retention, and Temperature-Triggered Reaction

Rona Chandrawati,[†] Leticia Hosta-Rigau,[†,‡,§] Dirk Vanderstraaten,[†] Shalitha A. Lokuliyana,[†] Brigitte Städler,[†] Fernando Albericio,[‡,§] and Frank Caruso[†,*]

[†]Centre for Nanoscience and Nanotechnology, Department of Chemical and Biomolecular Engineering, The University of Melbourne, Parkville, Victoria 3010 Australia, [‡]Institute for Research in Biomedicine, Barcelona Science Park, Baldiri Reixac 10-12, 08028-Barcelona, Spain, and [§]Department of Organic Chemistry, Martí i Franqués 1, University of Barcelona, 08028-Barcelona, Spain

ABSTRACT Advanced mimics of cells require a large yet controllable number of subcompartments encapsulated within a scaffold, equipped with a trigger to initiate, terminate, and potentially restart an enzymatic reaction. Recently introduced capsosomes, polymer capsules containing thousands of liposomes, are a promising platform for the creation of artificial cells. Capsosomes are formed by sequentially layering liposomes and polymers onto particle templates, followed by removal of the template cores. Herein, we engineer advanced capsosomes and demonstrate the ability to control the number of subcompartments and hence the degree of cargo loading. To achieve this, we employ a range of polymer separation layers and liposomes to form functional capsosomes comprising multiple layers of enzyme-loaded liposomes. Differences in conversion rates of an enzymatic assay are used to verify that multilayers of intact enzyme-loaded liposomes are assembled within a polymer hydrogel capsule. The size-dependent retention of the cargo encapsulated within the liposomal subcompartments during capsosome assembly and its dependence on environmental pH changes are also examined. We further show that temperature can be used to trigger an enzymatic reaction at the phase transition temperature of the liposomal subcompartments, and that the encapsulated enzymes can be utilized repeatedly in several subsequent conversions. These engineered capsosomes with tailored properties present new opportunities *en route* to the development of functional artificial cells.

KEYWORDS: capsosome · liposome multilayers · cargo retention · temperature-trigger

Biological cells are self-contained entities, equipped with multiple highly optimized and specialized organelles that have the ability to carry out specific metabolic activities. Artificial cells,[1−3] which are designed to mimic cellular functions, resemble biological cells but do not necessarily require their complexity. An important feature of artificial cells is the design of a compartmentalized assembly, which aims to perform a specific, spatially separated cellular function. Several systems have been reported, including vesosomes (liposomes inside a liposome),[4−7] polymerosomes within a polymerosome,[8] cellosomes (yeast cells associated with a polymer membrane),[9] dual-compartmentalized capsules,[10] and small polymer capsules within a large gel bead.[11] The uses of capsosomes,[12−15] liposomes[16−18] incorporated into a polymer carrier capsule,[19,20] are particularly promising subcompartmentalized assemblies as they combine the benefits of two fundamentally different systems. The polymer capsule, assembled *via* the sequential deposition of interacting polymers (*via* the layer-by-layer (LbL) technique[21−24]), provides the structural integrity of the construct/scaffold, while lowering control over the diffusion of (bio)molecules across the permeable polymer membrane. On the other hand, liposomes resemble the cell's organelles, with the potential to provide specialized subunits that allow for successive enzymatic reactions within a confined area. The assembly of capsosomes involves the deposition of a polymer precursor layer onto a sacrificial colloidal template, followed by the alternating assembly of liposomes and polymer separation layers. After the adsorption of a polymer capping layer, the membrane of the polymer carrier capsule is assembled and the template particle is removed. The optimized capsosome assembly employs cholesterol-modified polymers as a precursor, separation, and capping layer for the stable incorporation of the liposomes into the polymer film.[14,15] To date, we have reported nondegradable[12] and (bio)degradable[15] carrier capsules containing liposomes adsorbed through a maximum of two deposition steps. We have also demonstrated the retention of enzymatic cargo

*Address correspondence to fcaruso@unimelb.edu.au.

Received for review December 17, 2009 and accepted February 11, 2010.

Published online March 1, 2010.
10.1021/nn901843j

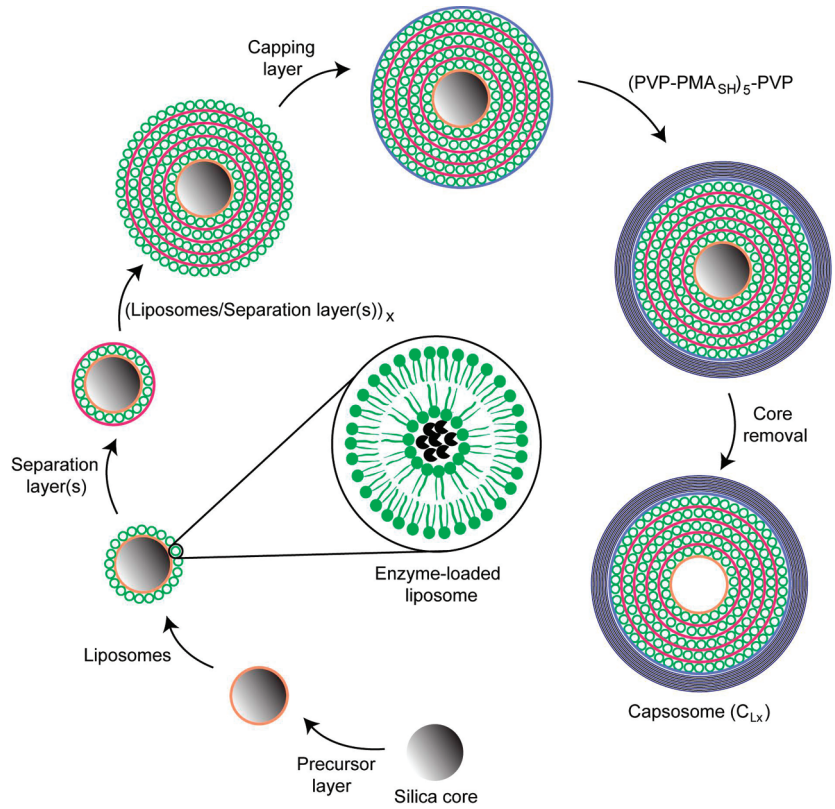

Scheme 1. Schematic illustration of capsosome assembly. A silica core is coated with a polymer precursor layer and liposomes, followed by the alternating adsorption of separation layer(s) and liposomes until the required number of layers is deposited. A polymer capping layer is adsorbed prior to the deposition of five bilayers of PVP and PMA$_{SH}$. Dissolution of the core results in a capsosome with multiple layers of intact (loaded) liposomes (C$_{Lx}$).

within the liposomal subcompartments[14] and the performance of a triggered enzymatic reaction upon lysis of the liposomes.[13] Furthermore, the ability of the capsosomes to encapsulate small hydrophobic cargo and their effect on the viability of colorectal cancer cells has been shown, and it has been confirmed that pristine capsosomes do not exhibit inherent cytotoxicity.[15]

In this paper, we investigate the essential and underlying parameters required to advance the design and performance of capsosomes. In particular, we (i) identify the upper limit of liposome multilayering onto particle templates with the aim to maximize the number of subcompartments and consequently the amount of loaded cargo; (ii) confirm the structural integrity and functionality of multiple layers of *intact* liposomes in a capsosome *via* an enzymatic assay; (iii) characterize the size-dependent retention of the cargo within the liposomes during the capsosome assembly process as a function of the environmental pH; and (iv) demonstrate that temperature can be used as a trigger to repeatedly initiate an enzymatic reaction without decomposition of the liposomal compartments.

Controlling the amount of loaded cargo per capsosome in a simple manner is essential for various applications, for example, the co-loading of enzymes for the performance of enzymatic cascade reactions in the same vessel. The assembly of multilayered subcompartments is performed by the alternating deposition of liposomes (*i.e.*, negatively charged or zwitterionic (L^- or L^{zw}) and unsaturated or saturated (L^u or L^s)) and polymer separation layers (*i.e.*, poly(L-lysine) (PLL), cholesterol-modified PLL (PLL$_c$), poly(methacrylic acid)-*co*-cholesteryl methacrylate (PMA$_c$), or a combination thereof) onto colloidal templates (Scheme 1). These polymers have previously been shown to allow for the subsequent deposition of liposomes in a second deposition step[15] and are expected to enable the multilayering of intact liposomes. Cholesterol, in particular, provides a widely applicable noncovalent anchor between polymer layers and liposomes.[14,25−27] The liposome/polymer assembly is then capped with PMA$_c$, followed by the sequential adsorption of poly(*N*-vinyl pyrrolidone) (PVP) and thiol-functionalized poly(methacrylic acid) (PMA$_{SH}$) to form the membrane of the polymer carrier capsule.[28] Upon cross-linking of the thiols in the polymer film and template core removal, capsosomes are obtained. To confirm the incorporation of multilayers of intact enzyme-loaded liposomal subcompartments within the PMA carrier capsules, a triggered colorimetric assay using β-lactamase[13] was conducted.

Cargo retention in a carrier vehicle is a crucial feature that governs the success of continuous enzymatic reactions as well as drug delivery approaches. Coencapsulation of different enzymes and/or small molecules re-

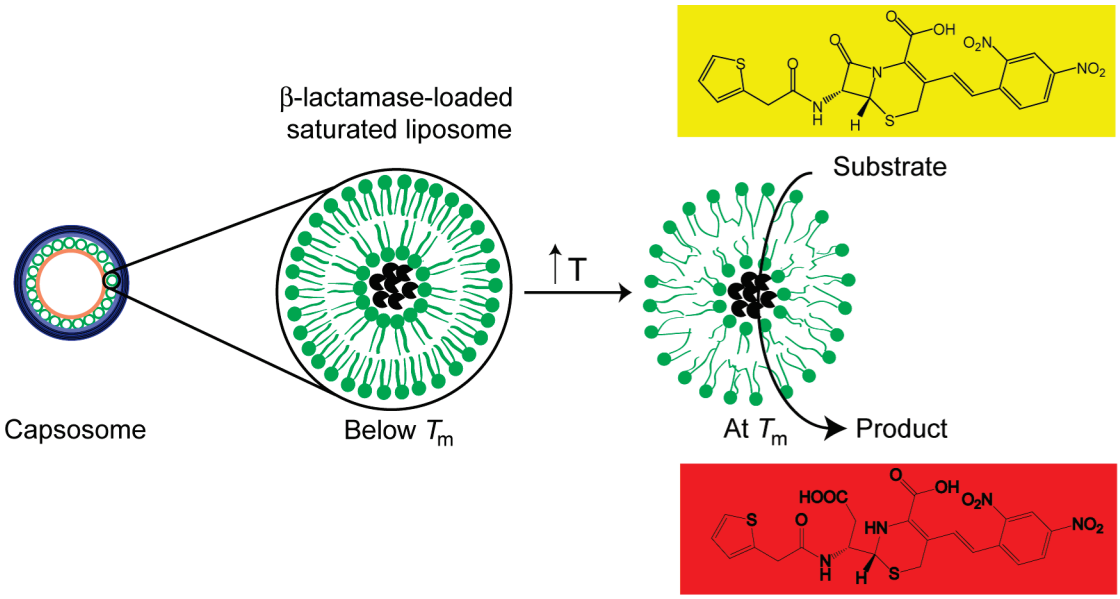

Scheme 2. Temperature-triggered enzymatic conversion. An increase in temperature to the phase transition temperature (T_m) of the liposomes results in a disordered liquid phase of the lipid membrane, allowing nitrocefin to cross the membrane to be hydrolyzed while retaining the β-lactamase inside the compartments.

quires an understanding of the size-dependent retention of different cargo in capsosomes, especially during their assembly. Although several studies have been reported on cargo encapsulation and the pH properties in liposomes, predominantly in solution,[29−31] there are different aspects that have to be taken into account when capsosomes are considered. In particular, effects attributed to the immobilization of liposomes to polymer-coated silica particle surfaces, that is, their anchoring to different cholesterol-modified polymers, as well as environmental pH changes during the capsosome assembly, have to be considered. In this study, we examine fluorescently labeled cargo of different sizes: luciferase fluorescein isothiocyanate (Luc_{FITC}, 79 000 Da), 10 000 Da dextran fluorescein isothiocyanate ($Dextran_{10\text{-}FITC}$), 4000 Da dextran fluorescein isothiocyanate ($Dextran_{4\text{-}FITC}$), carboxyrhodamine (CR, 550 Da), and carboxyfluorescein (CF, 400 Da). The pH-sensitive dye FITC was used to monitor the cargo retention and the pH changes within the liposomes simultaneously, while the pH-insensitive dye rhodamine was solely used to characterize cargo retention. The size range covers large molecules such as enzymes down to models for low molecular weight drugs.

A main challenge in designing artificial cells that can provide long-term therapeutic solutions for chronic diseases lies in the assembly of a system that contains functional and reusable enzymatic cargo trapped within compartments, which upon stimulating can be activated to convert molecules and simultaneously release the (therapeutic) products, provided there is a continuous supply of reactants. Thus far, the surfactant Triton X was used as an external trigger to initiate enzymatic reactions in capsosomes,[13] a trigger which causes lysis of the liposomes, but excludes the possibility to reuse the subunits. With the aim to repetitively use the enzymes trapped within the capsosomes, we exploit the enhanced permeability of the lipid membrane at the liquid−gel phase transition temperature (T_m) of the liposomes as a trigger to activate the enzymatic reaction by allowing the substrate to contact the enzymes (Scheme 2). Temperature-controlled permeability of lipid membranes can be tuned by employing liposomes with different lipid compositions and consequently different phase transition temperatures.[6,32] The temperature trigger does not require the introduction of harmful solutes/factors that might be harmful to the enzymatic cargo, and while it is less specific than ion channel (*e.g.*, gramicidin[33])-containing liposomes, it is a far simpler and robust approach. Although temperature-induced activation of liposomes has been previously used to initiate enzymatic reactions within liposome assemblies, it has not, to our knowledge, been considered in hierarchical liposome/polymer coassemblies. The close proximity to the polymer membrane, the incorporation of the cholesterol anchors into the lipid membrane, or the assembly process might potentially affect the properties of the lipid membrane. We examined the phase transition temperature as a trigger to activate a colorimetric reaction. Further, the retention and functionality of the enzymes within the liposomes over several reaction cycles were investigated.

RESULTS AND DISCUSSION

Liposome Multilayer Assembly onto 3 μm Silica Particles. Depending on the target application of the capsosomes, different types of liposomal subcompartments might be employed: charged or zwitterionic as well as saturated or unsaturated liposomes. For instance, the encapsulation of negatively charged or positively charged

cargo is likely to be facilitated by using zwitterionic or oppositely charged liposomes to prevent unfavorable interactions between the cargo and the subcompartments. Hence, we sought to identify different polymer separation layers to anchor various types of liposomes to a polymer film during multiple deposition steps. Successfully embedding cholesterol anchors into liposomes of different lipid composition can depend on the lipid composition *and* the moiety attached to the anchor.[27]

Multilayers of Negatively Charged Liposomes. The first approach to assemble liposome multilayers was performed by alternately adsorbing positively charged polymer separation layers (PLL_c or PLL) and negatively charged unsaturated or saturated liposomes ($L^{u,-}$ or $L^{s,-}$), thus expecting film growth driven by electrostatic interactions. The intensity of particles coated with fluorescently labeled liposomes was monitored by flow cytometry and the fluorescence intensity after the first liposome adsorption step was set to 100% and referred to as a single layer of liposomes.

To start the multilayer assembly, a polymer precursor layer, cholesterol-modified PLL (PLL_c) or pristine PLL, was adsorbed onto 3 μm-diameter silica particles. Both polymers have previously been proven to be suitable to adsorb a first layer of liposomes.[14,15] PLL_c, as a separation layer between the liposomes ($L^{u,-}$ or $L^{s,-}$), supported the consistent addition of a single layer of liposomes (~95%) in each adsorption step (Figure 1a, ★ and ☆). However, the number of alternating liposomes and PLL_c deposition steps was found to be limited; any additional exposure of the particles to a liposome solution did not result in further liposome adsorption but caused aggregation of the particles. The aggregation is likely caused by the multiple layers of liposomes affecting the colloidal stability of the particles. Moreover, the aggregation during the assembly of the saturated liposomes is possibly due to the temperature cycling between 37 °C for the liposome deposition steps and room temperature during the washing/centrifuging steps. On the other hand, using PLL as a separation layer only allowed for multiple liposome adsorption steps for $L^{s,-}$ but not for $L^{u,-}$ (Figure 1a, □ and ■). Taken together, these findings suggest that the adsorption of $L^{u,-}$ strongly relies on the presence of the cholesterol moieties, while the deposition of $L^{s,-}$ is predominantly electrostatically driven.

Aiming to confirm this hypothesis, we employed PMA_c, a negatively charged cholesterol-modified polymer, as a separation layer between the liposomes. (PMA was not considered since we previously demonstrated that unmodified PMA is not suitable to anchor liposomes into a polymer film.[14]) Using PMA_c as the separation layer enabled six deposition steps for $L^{u,-}$ before no further liposomal adsorption was observed (Figure 1b, ■). Multilayer assembly for the $L^{s,-}$ was not

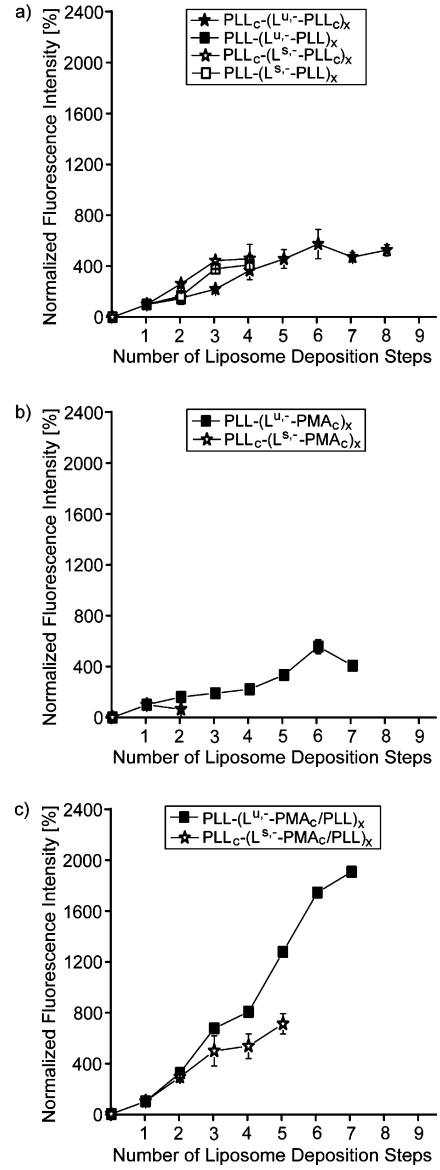

Figure 1. Multilayers of negatively charged liposomes. The fluorescence intensity of silica particles was measured by flow cytometry when PLL_c or PLL (a), PMA_c (b), or PMA_c/PLL (c) was used as polymer separation layers between the liposome deposition steps. Boost loading of unsaturated and saturated negatively charged liposomes, $L^{u,-}$ and $L^{s,-}$, was observed when PMA_c/PLL was employed as the separation layer (c).

observed when PMA_c was used as a separation layer (Figure 1b, ☆), neither at 23 °C nor at 41 °C (the T_m of 1,2-dipalmitoyl-*sn*-glycero-3-phosphocholine (DPPC), data not shown), confirming the unfavorable combination in assembling $L^{s,-}$ multilayers. Since only the cholesterol moieties are expected to anchor the liposomes to the polymer, these results support our hypothesis that $L^{s,-}$ requires electrostatic interaction with the polymer separation layer to enable liposome multilayer formation.

Interestingly, the use of PMA_c and PLL as a separation layer between the liposomes showed a synergistic loading effect (Figure 1c). While $L^{u,-}$ (Figure 1c, ■) and

$L^{s,-}$ (Figure 1c, ☆) were adsorbed in a similar amount during the first two deposition steps, the $L^{u,-}$ adsorption during the third adsorption step showed a ~400% increase in fluorescence, suggesting a high liposome loading. This assembly combination allowed for the anchoring of an equivalent amount of seven layers of liposomes in just three adsorption steps. This "boost-loading" of liposomes, particularly useful when a high loading of the same cargo is required, was also observed for the subsequent $L^{u,-}$ adsorption steps. The same effect was observed for $L^{s,-}$ but in a less pronounced manner. These results suggest that the combination of the two polymers PMA_c and PLL as separation layers is particularly well-suited for the assembly of multilayers of negatively charged liposomes due to the combined effect of electrostatically-driven adsorption and cholesterol-driven anchoring. A maximum of the equivalent of 20 single liposome layers could be assembled within seven deposition steps (Figure 1c, ■). We previously estimated that ~8000 liposomes are anchored to a PLL or PLL_c precoated 3 μm silica particle.[13] The measured fluorescence intensity after the first liposome deposition step was set as 100%. The increase in fluorescence intensity after multiple liposome deposition steps was used to estimate the approximate number of liposomal subcompartments per particle, leading to ~160 000 negatively charged liposomes assembled onto a 3 μm diameter silica particle after seven deposition steps, an amount far exceeding what we[15] and others[34] have so far reported.

Multilayers of Zwitterionic Liposomes. Multilayers of zwitterionic liposomes were assembled using the same set of polymer separation layers as previously described. Independent of the type of liposomes, PLL_c, PLL, and PMA_c/PLL as a separation layer did not allow for liposome multilayer assembly (Figure 2a,c). However, as depicted in Figure 2b, a constant increase in liposomal payload was observed when only PMA_c was used as a separation layer (Figure 2b, ★ and ☆). Using PMA_c and PLL_c as alternating separation layers only allowed additional liposome deposition after a PMA_c layer (Figure 2b, ■ and □), suggesting that the assembly of zwitterionic liposomes is predominantly driven by the cholesterol anchoring. The multilayer assembly of $L^{u,zw}$ or $L^{s,zw}$ with PMA_c as a separation layer enables the "stepwise loading" of liposomes, an approach applicable for entrapping equivalent amounts of multicargo in a single capsosome (*e.g.*, for enzymatic cascade reactions or controlled dosage for drug co-delivery approaches).

Capsosome Assembly. Capping the liposome (multilayer) assembly with PMA_c, subsequent deposition of PVP and PMA_{SH} to form the membrane of the carrier vehicle, cross-linking of the thiols in the polymer film, and removal of the template core yields capsosomes. Capsosomes prepared with one or eight $L^{s,zw}$ deposition steps, C_{L1} or C_{L8}, respectively, were visualized using optical and electron microscopy techniques to confirm and

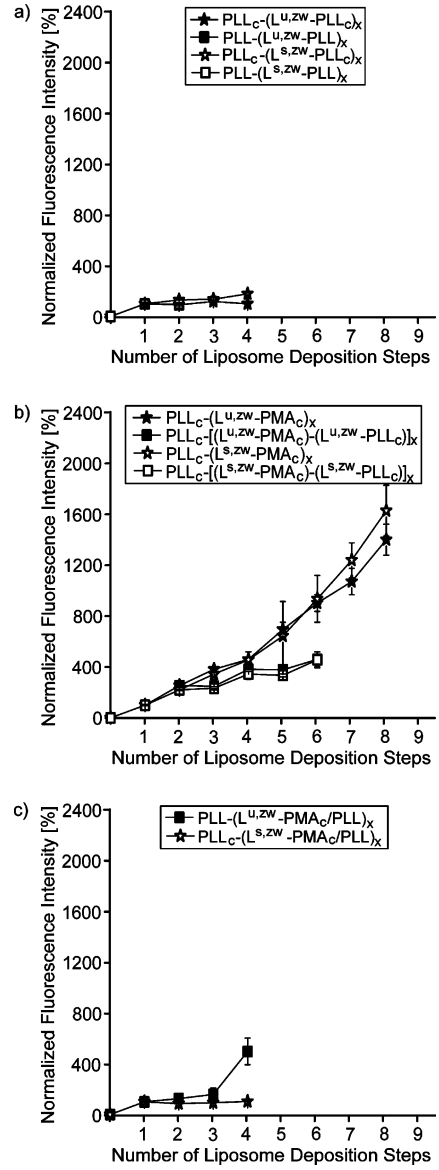

Figure 2. Multilayers of zwitterionic liposomes. The fluorescence intensity of silica particles was measured by flow cytometry when PLL_c or PLL (a), PMA_c (b), or PMA_c/PLL (c) was used as polymer separation layers between the liposome deposition steps. Stepwise loading of unsaturated and saturated zwitterionic liposomes, $L^{u,zw}$ and $L^{s,zw}$, was observed when PMA_c was used as the separation layer (b).

compare their appearance and structural integrity (Figure 3). Differential interference contrast (DIC) images taken under physiological conditions demonstrated that both types of capsosomes were intact and non-agglomerated and preserved the spherical shape of the template silica particles (Figure 3a,b). Moreover, confocal laser scanning microscopy (CLSM) images of capsosomes assembled using fluorescently labeled liposomes confirmed the presence of additional liposome layers for C_{L8} by the observation of a thicker shell and consequently the larger diameter of 5.01 ± 0.46 μm (Figure 3d) compared to 3.55 ± 0.30 μm for C_{L1} (Figure 3c). This difference is expected assuming that intact 50 nm liposomes were loaded in eight adsorption steps (~16 lay-

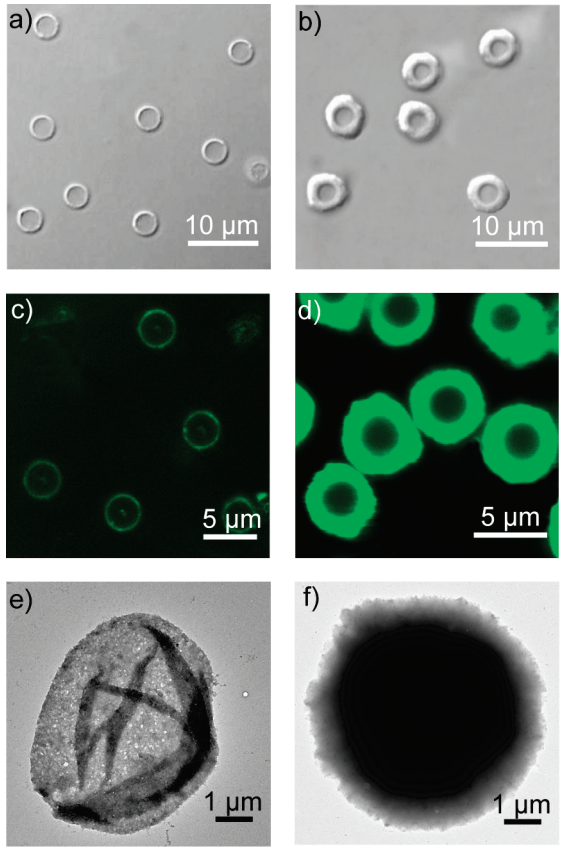

Figure 3. Structural integrity of capsosomes with stepwise-loaded liposomes ($L^{S,ZW}$, PMA_c separation layer). DIC images of capsosomes with one (C_{L1}) (a) and eight (C_{L8}) (b) liposome deposition steps. CLSM images confirmed the higher liposome loading for C_{L8} (d) in comparison to C_{L1} (c). TEM images show the typical folded carrier capsule of a C_{L1} (e) in comparison to the particle-like appearance of the C_{L8} due to its high liposomal payload (f).

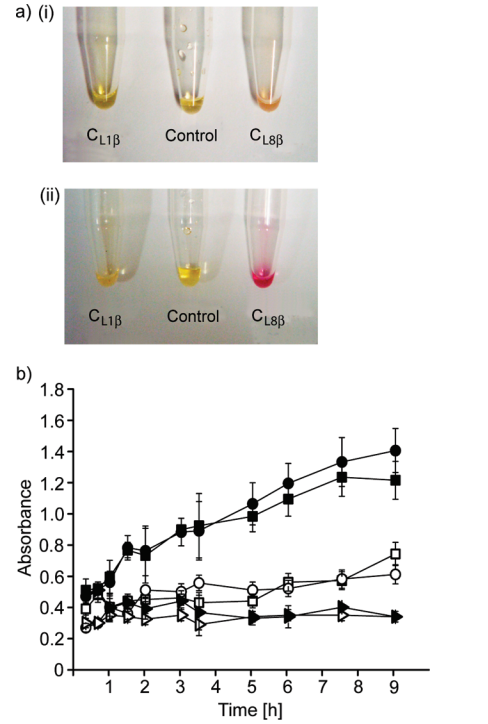

Figure 4. Enzymatic conversion rates of capsosomes with stepwise β-lactamase-loaded liposomes ($L^{S,ZW}$, PMA_c separation layer). (a) Photographs taken after 2 h (i) and 9 h (ii) of C_{L1} and C_{L8} containing β-lactamase-loaded liposomes, $C_{L1\beta}$ and $C_{L8\beta}$, respectively, exposed to TX (left and right tubes) and $C_{L8\beta}$ in the absence of TX (middle tube). (b) Absorbance measurements of the quantitative β-lactamase assay using core−shell particles (□ and ■) and capsosomes (○ and ●) assembled with one or eight liposome deposition steps (open or closed symbols, respectively) with TX. Controls without the addition of TX are also shown (empty arrowhead and solid arrowhead).

ers of liposomes, Figure 2b, ☆), resulting in the addition of ~1.6 μm in diameter for C_{L8}, in comparison to C_{L1}. Transmission electron microscopy (TEM) images further supported the presence of a high liposomal loading for C_{L8}; while C_{L1} showed the expected folding of the polymer carrier capsule (Figure 3e), C_{L8} remained spherically intact and appeared particle-like (Figure 3f). This observation demonstrates that one layer of liposomes is not sufficient to stabilize the polymer membrane, that is, to keep the capsosomes in their spherical shape under vacuum, while multiple layers of liposomes sustain the capsosomes' shape even under vacuum.

To confirm the presence of multiple intact enzyme-loaded liposomal subcompartments within the PMA capsules and that the amount of loaded cargo can be simply controlled by the number of deposited liposome layers, the enzymatic conversion rates of capsosomes assembled with β-lactamase-loaded liposomes in one or eight deposition steps, $C_{L1\beta}$ or $C_{L8\beta}$, were compared. β-Lactamase, an enzyme which converts the yellow substrate nitrocefin into its red hydrolyzed product, has previously been used to demonstrate the functionality of capsosomes by performing a triggered quantitative enzymatic colorimetric assay.[13] The enzymatic reaction only occurred when the β-lactamase-loaded liposomes were lysed using the surfactant Triton X (TX) (Figure 4a (i) after 2 h and (ii) after 9 h, left ($C_{L1\beta}$) and right ($C_{L8\beta}$) tubes), while in the absence of TX, no reaction occurred (Figure 4a, middle tubes ($C_{L8\beta}$)), verifying the presence of intact (multiple) layers of liposomes loaded with active enzymatic cargo within the capsosomes. While there was a clear difference in enzymatic conversion rate measured by UV−vis spectrophotometry over time, which confirmed the different amount of loaded active enzymatic cargo within $C_{L1\beta}$ and $C_{L8\beta}$ and in the corresponding core−shell particles (Figure 4b), the difference was lower than expected; after 9 h, $C_{L8\beta}$ was 2.5× faster compared to $C_{L1\beta}$. This discrepancy could be explained by a low encapsulation efficiency of the enzymes within the liposomes and/or the presence of empty liposomes, an observation which has recently been reported by Lohse *et al.*[35]

Cargo Retention within the Liposomal Subcompartments. Apart from gaining control over the number of assembled liposomal subcompartments, understanding the environmental changes within the liposomes as

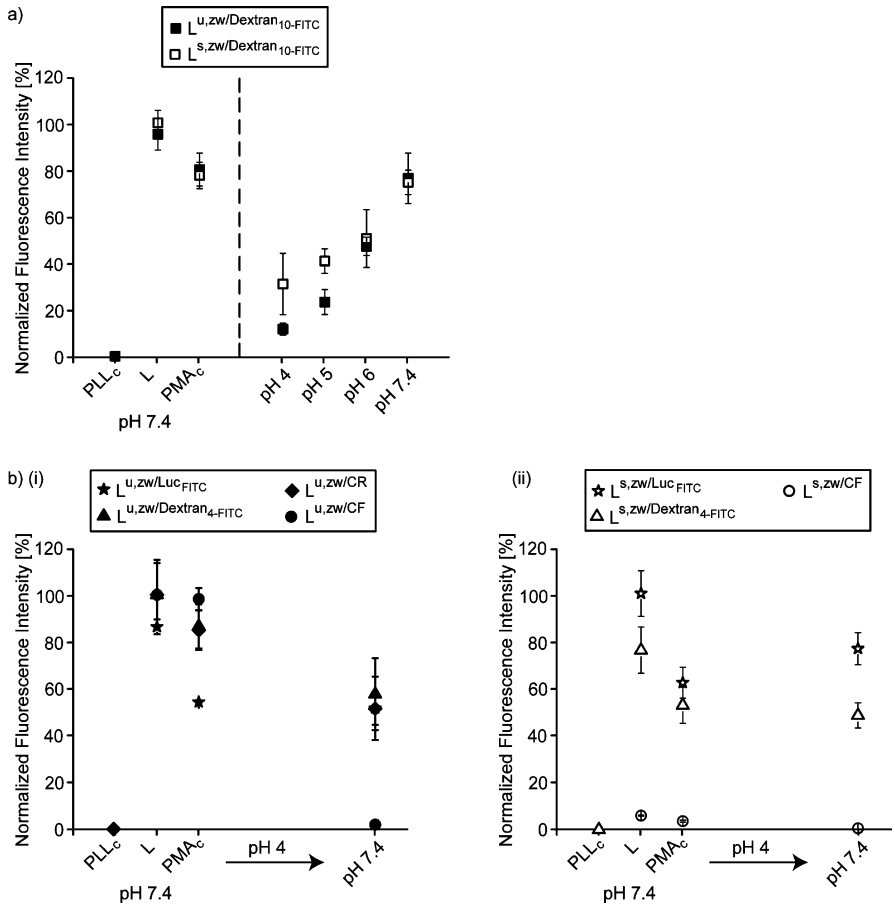

Figure 5. Cargo size-dependent retention. (a) Normalized fluorescence intensity of silica particles measured by flow cytometry, due to the encapsulation of Dextran$_{10\text{-FITC}}$ (10 000 Da) within the zwitterionic liposomes, during capsosome assembly followed by exposure to buffer solutions with pH between 4 and 7.4. (b) Summary of cargo size-dependent retention for zwitterionic unsaturated ($L^{u,zw}$) (i) and saturated ($L^{s,zw}$) (ii) liposomes encapsulating Luc$_{FITC}$ (79 000 Da), Dextran$_{4\text{-FITC}}$ (4000 Da), carboxyrhodamine (CR, 550 Da), or carboxyfluorescein (CF, 400 Da) during capsosome assembly.

well as the cargo retention properties is crucial. To simultaneously monitor the pH changes within the liposomes and to identify the lower limit of the size of cargo that can be encapsulated, we entrapped cargo of different molecular weights coupled to the pH-sensitive fluorophore fluorescein isothiocyanate (FITC) within liposomes. The fluorescence intensity of silica particles was measured upon assembly of a PLL$_c$ precursor layer, the cargo-loaded liposomes, and a PMA$_c$ capping layer under physiological conditions (HEPES buffer, pH 7.4). Other assembly conditions were found to be unfavorable for either the amount of adsorbed liposomes or the cargo retention (see Supporting Information, Figure S1). We then exposed the assemblies to buffer solutions with pH between 4 and 7.4. This pH range was chosen because the assembly and cross-linking of the polymer membrane requires buffer solutions at pH 4 and 6, respectively.

Figure 5a depicts an example of such an experiment using Dextran$_{10\text{-FITC}}$ encapsulated within zwitterionic liposomes ($L^{u,zw}$, ■, and $L^{s,zw}$, □). After capping the liposomes with PMA$_c$ in pH 7.4, the buffer solution was changed from HEPES (pH 7.4) to NaOAc (pH 4), which caused a decrease in fluorescence intensity, suggesting that the pH within the liposomes was lowered. The environmental change within the liposomes was further supported by a stepwise increase in intensity upon returning the environmental pH back from 4 to 7.4. Nevertheless, when returned to pH 7.4, the measured intensity was the same as before the pH changes, suggesting that there was no measurable loss of cargo from the liposomes. Although the environmental changes within the liposomes currently cannot be avoided, we note that the (bio)molecules are only exposed to such pH changes during the assembly process.

Figure 5b summarizes the cargo retention of Luc$_{FITC}$, Dextran$_{4\text{-FITC}}$, CR, and CF entrapped within zwitterionic unsaturated ($L^{u,zw}$, Figure 5b(i)) and zwitterionic saturated ($L^{s,zw}$, Figure 5b(ii)) liposomes after liposome deposition onto PLL$_c$ precoated silica particles, and after capping with PMA$_c$ and exposure to different pH. (For the negatively charged liposomes $L^{u,-}$ and $L^{s,-}$, see Supporting Information, Figure S2.) The data suggest that, during the liposome deposition (pH 7.4), both types of liposomes are similarly well-suited to encapsulate cargo down to 550 Da. However, only $L^{u,zw}$ could retain small-sized cargo (*i.e.*, CF, $<$500 Da) during the initial liposome adsorption step. The necessity of raising

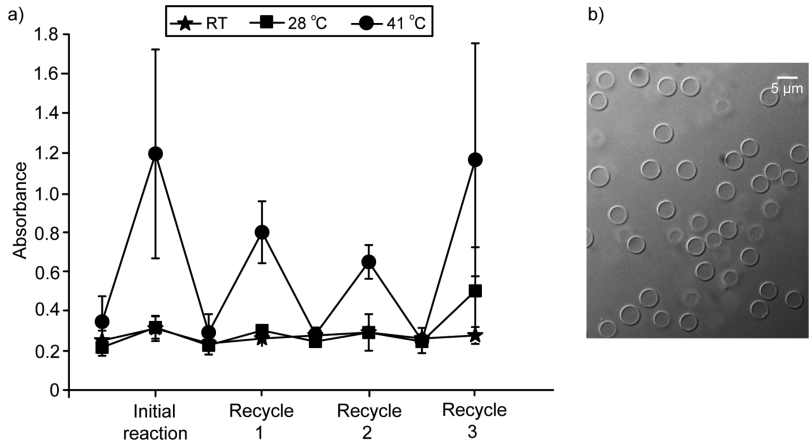

Figure 6. Temperature-triggered enzymatic reaction in reusable capsosomes. (a) Absorbance readings of an enzymatic assay using capsosomes with β-lactamase-loaded DPPC liposomes ($C_{L(DPPC)-\beta}$) incubated at room temperature (23 °C) (★), 28 °C (■), or 41 °C (●). The enzymatic conversion was only observed when the capsosomes were incubated at the phase transition temperature (T_m) of the liposomal subunits. The retention of the functional enzymes inside of the liposomal subcompartments was confirmed by repetitively performing the temperature-induced assay. (b) DIC image of capsosomes after being reused four times.

the temperature above T_m[14] during the assembly of the saturated liposomes likely caused the loss of the cargo. The cargo (with the exception of Luc_{FITC}) entrapped in $L^{u,zw}$ remained unaffected by capping with PMA_c, while ~30−40% of the cargo encapsulated within $L^{s,zw}$ was lost, again most likely due to the required cycling above T_m for the PMA_c adsorption. On the other hand, upon pH cycling from 7.4 to 4 and back to 7.4, a ~20 and 35% cargo loss for $Dextran_{4\text{-}FITC}$ and CR was monitored, respectively, from $L^{u,zw}$, while the cargo within $L^{s,zw}$ was largely retained despite the pH cycling. Additionally, even though unsaturated liposomes were able to encapsulate CF during the initial stages of the assembly (at physiological conditions), there was no restoration of the fluorescence intensity observed when the pH was raised from 4 back to 7.4, suggesting the entire release of the cargo from the liposomes occurred due to exposure to the acidic environment. This retention characteristic suggests that, when exposure to an acidic environment is required for the capsosome assembly, the cutoff size for the cargo encapsulated within the liposomes is between the molecular size of CF and CR (*i.e.*, between 400 and 550 Da). It was previously reported that the presence of weak acids,[36] in this case acetic acid, or fetal bovine serum[37] can induce the release of encapsulated CF from liposomes.

While the change in permeability of the lipid membrane due to the increased temperature or the presence of weak acids has to be considered for the assembly of capsosomes loaded with small cargo, this feature might be beneficial for biomedical applications, that is, for the performance of continuous enzymatic reactions or for the slow release of small drugs in the acidic intracellular compartments.

Temperature-Triggered Enzymatic Reaction. To demonstrate that the enhanced permeability of the lipid membrane at T_m can be used as a trigger to initiate an enzymatic reaction without destruction of the liposomal subcompartments, we assembled capsosomes containing β-lactamase-loaded DPPC liposomes ($L_{DPPC-\beta}$, T_m = 41 °C). Upon an increase of the temperature to the T_m of the liposomes, the substrate nitrocefin is able to cross the lipid membrane, and be hydrolyzed into its red product and released from the compartment again (Scheme 2). The capsosomes were incubated at room temperature (RT, 23 °C), at 28 and 41 °C, and the enzymatic conversion rate was followed over time (Figure 6a). The enzymatic conversion was only observed for capsosomes incubated at 41 °C, but not at RT or at 28 °C. Hence, although anchored to the polymer film, the saturated liposomes provide an effective diffusion barrier for nitrocefin below their phase transition temperature.

Further, to confirm that the temperature-triggered approach neither destructs the liposomal subcompartments nor causes the release of the enzymes, we repeated the enzymatic conversion by replacing the hydrolyzed nitrocefin with fresh substrate over several cycles. The enzymatic conversion occurred at a similar rate to that observed for three cycles (Figure 6a), indicating that (i) β-lactamase was retained inside the liposomes, (ii) the reinitiation of the reaction is possible, and (iii) there is no loss of functional activity of the enzymes. The capsosomes, after repetitive exposure to elevated temperatures, preserved their structural integrity (Figure 6b).

In summary, the repetitive temperature-triggered activation of the enzymatic conversion provides unprecedented success in microencapsulated biocatalysis using a subcompartmentalized system and has the potential to control an enzymatic reaction, where the initiation/termination of several reaction steps is required.

CONCLUSIONS

We have reported three essential aspects regarding the assembly and functionality of capsosomes. We have demonstrated that the number of subcompartments within a capsosome can be controlled by the alternate layering of liposomes and polymer separation layers. A maximum of ~160 000 subcompartments (equivalent to 20 single liposome layers) could be assembled with seven deposition steps on 3 μm diameter templates. An enzymatic reaction confirmed the assembly of multiple layers of intact liposomes within a capsosome. We determined that cargo trapped within $L^{u,zw}$ was predominantly lost during pH cycling, while cargo encapsulated within $L^{s,zw}$ was mainly lost during capping with PMA_c. In the case when acidic pH conditions are required during the capsosome assembly, the cutoff size of (bio)molecules that can be encapsulated with more than 50% retention efficiency within the liposomal subcompartment has been identified to be ~500 Da. For the first time, we demonstrated the reuse of enzymes trapped within the liposomal subcompartments of a capsosome by using temperature as a trigger to initiate the enzymatic reaction. The reported results point to capsosomes being a promising platform toward the creation of therapeutic artificial cells and organelles.

EXPERIMENTAL SECTION

Materials. Poly(L-lysine) (PLL, M_w 40 000−60 000), poly(*N*-vinyl pyrrolidone) (PVP, M_w 10 000), β-lactamase, luciferase (from *Vibrio fischeri*), fluorescein isothiocyanate (FITC), $Dextran_{10\text{-}FITC}$ (M_w 10 000), $Dextran_{4\text{-}FITC}$ (M_w 4000), carboxyrhodamine (CR, M_w 550), carboxyfluorescein (CF, M_w 400), 4-(2-hydroxyethyl)piperazine-1-ethanesulfonic acid (HEPES), sodium chloride (NaCl), sodium acetate (NaOAc), 2-(*N*-morpholino)ethanesulfonic acid (MES), and chloroform were purchased from Sigma-Aldrich. Silica particles (3.25 μm diameter) were purchased from Microparticles GmbH, Germany. Zwitterionic lipids, [1,2-dioleoyl-*sn*-glycero-3-phosphocholine (DOPC, phase transition temperature −4 °C), 1,2-dimyristoyl-*sn*-glycero-3-phosphocholine (DMPC, phase transition temperature 24 °C), 1,2-dipalmitoyl-*sn*-glycero-3-phosphocholine (DPPC, phase transition temperature 41 °C)], negatively charged lipids, [1,2-dioleoyl-*sn*-glycero-3-(phospho-L-serine) (DOPS, phase transition temperature −4 °C)], and fluorescent lipids [1-oleoyl-2-[6-[(7-nitro-2−1,3-benzoxadiazol-4-yl)amino]hexanoyl]-*sn*-glycero-3 phosphocholine (NBD-PC)] were purchased from Avanti Polar Lipids, USA. 1,8-Bismaleimidodiethyleneglycol ($BM(PEG)_2$) was purchased from Thermo Fisher, USA.

Cholesterol-modified poly(L-lysine) (PLL_c, M_w 40 000−60 000) and poly(methacrylic acid)-*co*-(cholesteryl methacrylate) (PMA_c, M_w 11 560) were synthesized according to a previously published protocol.[14]

Thiol-functionalized poly(methacrylic acid) (PMA_{SH}) with 14 mol % of thiol groups was synthesized as previously reported.[38]

Poly(methacrylic acid) with 6 mol % of pyridyl disulfide activated thiol groups (PMA_{PD}) was synthesized according to a previously published protocol.[20]

Liposome Formation. Unilamellar liposomes were prepared by evaporation of the chloroform of the lipid solution (2.5 mg of DOPC ($L^{u,zw}$), DOPC/DOPS = 4:1 ($L^{u,-}$), DMPC/DPPC = 4:1 ($L^{s,zw}$), or DMPC/DPPC/DOPS = 7:1:2 ($L^{s,-}$)) under nitrogen for 1 h, followed by hydration with 0.6 mg β-lactamase or Luc_{FITC} dissolved in 200 μL of HEPES buffer (10 mM HEPES, 150 mM NaCl, pH 7.4). The concentration of $Dextran_{10\text{-}FITC}$, $Dextran_{4\text{-}FITC}$, or CF encapsulated within the liposomes was 1 mM, while CR was encapsulated with a concentration of 60 mM. For fluorescently labeled liposomes, 1 wt % of NBD-PC was added to the lipid solution. Each solution was diluted into 1 mL of HEPES buffer and extruded through 50 nm filters 31 times to obtain liposomes of monodisperse size.

Capsosome Assembly. A suspension of SiO_2 particles (5 wt %) in HEPES buffer was incubated with the polymer precursor layer, PLL_c or PLL (1 mg mL^{-1}, 15 min), and washed three times (1060*g*, 30 s). From hereon, the samples were covered with aluminum foil to avoid the exposure of the fluorescent dyes to light and possible photobleaching. Liposomes (1.25 mg mL^{-1}, 40 min) were allowed to interact with the polymer-coated particles, washed three times, and polymer separation layers were subsequently adsorbed (1 mg mL^{-1}, 15 min). The adsorption of liposomes and polymer separation layer(s) was repeated until the required number of layers was deposited, followed by the adsorption of a PMA_c capping layer (1 mg mL^{-1}, 15 min). The fluorescence of the particles was analyzed by flow cytometry after each liposome adsorption step. The buffer was changed to NaOAc (20 mM NaOAc, pH 4.0), and five bilayers of alternating PVP (1 mg mL^{-1}, 10 min) and PMA_{SH} (1 mg mL^{-1}, 10 min) were sequentially deposited. The thiols within the polymer layers were cross-linked with either PMA_{PD} (1 mg mL^{-1}, 15 h) in NaOAc buffer or $BM(PEG)_2$ (2 mM, 15 h) in MES buffer (50 mM MES, pH 6.0). $BM(PEG)_2$ cross-linked capsosomes were only used for the temperature triggered enzymatic reaction. Capsosomes were formed by dissolving the silica core particles using a 2 M HF/8 M NH_4F solution for 2 min, followed by multiple centrifugation (4500*g*, 3 min)/NaOAc buffer washing cycles.

Flow Cytometry. A Cyflow Space (Partec GmbH) flow cytometer using an excitation wavelength of 488 nm was used to measure the intensity of the liposome-coated particles. At least 20 000 particles were analyzed in each experiment. The alternating deposition of polymer(s) and liposomes onto silica particles (with the aim to assemble liposome multilayers) was characterized using flow cytometry. After each liposome deposition step, the fluorescence intensity of the particles was monitored, and when there was no increase in fluorescence intensity, an increase lower than 50%, or severe aggregation, no further deposition steps were performed. At least two independent experiments were performed.

Differential Interference Contrast (DIC) Microscopy. DIC images of capsosomes were taken with an Olympus IX71 digital wide-field microscope equipped with a DIC slider (U-DICT, Olympus), the corresponding filter sets and a 60× oil immersion objective.

Confocal Laser Scanning Microscopy (CLSM). Fluorescently labeled capsosomes were imaged with a Leica TCS SP2 AOBS confocal microscope equipped with an argon laser (λ = 488 nm) using a 63× oil immersion objective (Leica, Germany).

Transmission Electron Microscopy (TEM). Five microliters of the capsosome sample was adsorbed for 2 min onto a carbon-coated Formvar film mounted on 300 mesh plasma-treated copper grids (ProSciTech, Australia). The grids were blotted and investigations were undertaken using an FEI Company Tecnai TF30 (FEI-Company, Eindhoven, The Netherlands) instrument.

Enzymatic Hydrolysis of Nitrocefin by β-Lactamase in Capsosomes. A suspension of 3×10^7 particles or capsosomes/mL was allowed to interact with 50 μg mL^{-1} nitrocefin. Triton X (TX) was subsequently added at a final concentration of 0.5% (v/v). An increase in the hydrolyzed product of nitrocefin was followed over time through monitoring absorbance readings at 492 nm using a NanoDrop 1000 spectrophotometer (Thermo Fisher Scientific).

Cargo Retention in Capsosomes. A suspension of SiO_2 particles (5 wt %) in HEPES buffer was incubated with the polymer precursor layer PLL_c (1 mg mL^{-1}, 15 min) and washed three times (1060*g*, 30 s). Liposomes encapsulating different cargo (1.25 mg mL^{-1}, 40 min) were allowed to interact with the polymer-coated particles, washed three times, and the fluorescence intensity was measured by flow cytometry. The polymer capping layer

PMA_c was subsequently adsorbed (1 mg mL^{-1}, 15 min), followed by further washing. The assembly took ~100 min. The fluorescence intensity of the particles was monitored before and after exposure to pH varying for ~5 min.

Temperature-Triggered and Cycling of the Enzymatic Hydrolysis of Nitrocefin in Capsosomes. The capsosome−nitrocefin suspension was incubated at room temperature (23 °C) or 28 or 41 °C. Absorbance readings were monitored over time at 492 nm using a NanoDrop1000 spectrophotometer (Thermo Fisher Scientific) to follow the progression of nitrocefin hydrolysis. The capsosomes were centrifuged (4500*g*, 3 min), and the supernatant (the hydrolyzed product) was removed and replaced with fresh nitrocefin, followed by incubation at a given temperature and absorbance readings.

Acknowledgment. This work was supported by the Australian Research Council under the Federation Fellowship (F.C.) and Discovery Project (F.C.) schemes. We thank Dr. A. D. Price (The University of Melbourne) for assisting in cross-linking the PMA_{SH} using $BM(PEG)_2$ and labeling luciferase-FITC, Dr. A. Postma (CSIRO Molecular and Health Technologies) for his help in PMA_c synthesis, and Dr. A. N. Zelikin (The University of Melbourne) and S.-F. Chong (The University of Melbourne) for their input in assembling the PMA hydrogel carrier capsules.

Supporting Information Available: Flow cytometry experiments on the encapsulation of CR within zwitterionic liposomes on silica particles; flow cytometry experiments on cargo size-dependent retention for negatively charged liposomes during capsosome assembly. This material is available free of charge *via* the Internet at http://pubs.acs.org.

REFERENCES AND NOTES

1. Drubin, D. A.; Way, J. C.; Silver, P. A. Designing Biological Systems. *Genes Dev.* **2007**, *21*, 242–254.
2. Deamer, D. A Giant Step towards Artificial Life. *Trends Biotechnol.* **2005**, *23*, 336–338.
3. Mann, S. Life as a Nanoscale Phenomenon. *Angew. Chem., Int. Ed.* **2008**, *47*, 5306–5320.
4. Kisak, E. T.; Coldren, B.; Evans, C. A.; Boyer, C.; Zasadzinski, J. A. The Vesosome—A Multicompartment Drug Delivery Vehicle. *Curr. Med. Chem.* **2004**, *11*, 199–219.
5. Boyer, C.; Zasadzinski, J. A. Multiple Lipid Compartments Slow Vesicle Contents Release in Lipases and Serum. *ACS Nano* **2007**, *1*, 176–182.
6. Bolinger, P. Y.; Stamou, D.; Vogel, H. An Integrated Self-Assembled Nanofluidic System for Controlled Biological Chemistries. *Angew. Chem., Int. Ed.* **2008**, *47*, 5544–5549.
7. Mishra, V.; Mahor, S.; Rawat, A.; Dubey, P.; Gupta, P. N.; Singh, P.; Vyas, S. P. Development of Novel Fusogenic Vesosomes for Transcutaneous Immunization. *Vaccine* **2006**, *24*, 5559–5570.
8. Chiu, H. C.; Lin, Y. W.; Huang, Y. F.; Chuang, C. K.; Chern, C. S. Polymer Vesicles Containing Small Vesicles within Interior Aqueous Compartments and pH-Responsive Transmembrane Channels. *Angew. Chem., Int. Ed.* **2008**, *47*, 1875–1878.
9. Fakhrullin, R. F.; Paunov, V. N. Fabrication of Living Cellosomes of Rod-like and Rhombohedral Morphologies Based on Magnetically Responsive Templates. *Chem. Commun.* **2009**, 2511–2513.
10. Kreft, O.; Skirtach, A. G.; Sukhorukov, G. B.; Möhwald, H. Remote Control of Bioreactions in Multicompartment Capsules. *Adv. Mater.* **2007**, *19*, 3142–3145.
11. De Geest, B. G.; De Koker, S.; Immesoete, K.; Demeester, J.; De Smedt, S. C.; Hennink, W. E. Self-Exploding Beads Releasing Microcarriers. *Adv. Mater.* **2008**, *20*, 3687–3691.
12. Städler, B.; Chandrawati, R.; Goldie, K.; Caruso, F. Capsosomes: Subcompartmentalizing Polyelectrolyte Capsules Using Liposomes. *Langmuir* **2009**, *25*, 6725–6732.
13. Städler, B.; Chandrawati, R.; Price, A. D.; Chong, S.-F.; Breheney, K.; Postma, A.; Connal, L. A.; Zeilikin, A. N.; Caruso, F. A Microreactor with Thousands of Subcompartments: Enzyme-Loaded Liposomes within Polymer Capsules. *Angew. Chem., Int. Ed.* **2009**, *48*, 4359–4362.
14. Chandrawati, R.; Städler, B.; Postma, A.; Connal, L. A.; Chong, S.-F.; Zelikin, A. N.; Caruso, F. Cholesterol-Mediated Anchoring of Enzyme-Loaded Liposomes within Disulfide-Stabilized Polymer Carrier Capsules. *Biomaterials* **2009**, *30*, 5988–5998.
15. Hosta-Rigau, L.; Städler, B.; Yan, Y.; Nice, E.; Heath, J.; Albericio, F.; Caruso, F. Capsosomes with Multilayered Subcompartments: Assembly and Loading with Hydrophobic Cargo. *Adv. Funct. Mater.* **2010**, *20*, 59–66.
16. Noireaux, V.; Libchaber, A. A Vesicle Bioreactor as a Step toward an Artificial Cell Assembly. *Proc. Natl. Acad. Sci. U.S.A.* **2004**, *101*, 17669–17674.
17. Torchilin, V. P. Recent Advances with Liposomes as Pharmaceutical Carriers. *Nat. Rev. Drug Discovery* **2005**, *4*, 145–160.
18. Christensen, S. M.; Stamou, D. Surface-Based Lipid Vesicle Reactor Systems: Fabrication and Applications. *Soft Matter* **2007**, *3*, 828–836.
19. Städler, B.; Price, A. D.; Chandrawati, R.; Hosta-Rigau, L.; Zeilikin, A. N.; Caruso, F. Polymer Hydrogel Capsules: *En Route* toward Synthetic Cellular Systems. *Nanoscale* **2009**, *1*, 68–73.
20. Chong, S.-F.; Chandrawati, R.; Städler, B.; Park, J.; Cho, J.; Wang, Y.; Jia, Z.; Bulmus, V.; Davis, T. P.; Zeilikin, A. N.; Caruso, F. Stabilization of Polymer−Hydrogel Capsules *via* Thiol−Disulfide Exchange. *Small* **2009**, *5*, 2601–2610.
21. De Geest, B. G.; De Koker, S.; Sukhorukov, G. B.; Kreft, O.; Parak, W. J.; Skirtach, A. G.; Demeester, J.; De Smedt, S. C.; Hennink, W. E. Polyelectrolyte Microcapsules for Biomedical Applications. *Soft Matter* **2009**, *5*, 282–291.
22. De Koker, S.; De Geest, B. G.; Singh, S. K.; De Rycke, R.; Naessens, T.; Van Kooyk, Y.; Demeester, J.; De Smedt, S. C.; Grooten, J. Polyelectrolyte Microcapsules as Antigen Delivery Vehicles to Dendritic Cells: Uptake, Processing, and Cross-Presentation of Encapsulated Antigens. *Angew. Chem., Int. Ed.* **2009**, *48*, 8485–8489.
23. Quinn, J. F.; Johnston, A. P. R.; Such, G. K.; Zelikin, A. N.; Caruso, F. Next Generation, Sequentially Assembled Ultrathin Films: Beyond Electrostatics. *Chem. Soc. Rev.* **2007**, *36*, 707–718.
24. De Geest, B. G.; Sanders, N. N.; Sukhorukov, G. B.; Demeester, J.; De Smedt, S. C. Release Mechanisms for Polyelectrolyte Capsules. *Chem. Soc. Rev.* **2007**, *36*, 636–649.
25. Svedhem, S.; Pfeiffer, I.; Larsson, C.; Wingren, C.; Borrebaeck, C.; Höök, F. Patterns of DNA-Labeled and scFv-Antibody-Carrying Lipid Vesicles Directed by Material-Specific Immobilization of DNA and Supported Lipid Bilayer Formation on an Au/SiO_2 Template. *ChemBioChem* **2003**, *4*, 339–343.
26. Lee, S.-M.; Chen, H.; Dettmer, C. M.; O'Halloran, T. V.; Nguyen, S. T. Polymer-Caged Lipsomes: A pH-Responsive Delivery System with High Stability. *J. Am. Chem. Soc.* **2007**, *129*, 15096–15097.
27. Beales, P. A.; Vanderlick, T. K. Partitioning of Membrane-Anchored DNA between Coexisting Lipid Phases. *J. Phys. Chem. B* **2009**, *113*, 13678–13686.
28. Zelikin, A. N.; Li, Q.; Caruso, F. Disulfide-Stabilized Poly(methacrylic acid) Capsules: Formation, Cross-Linking, and Degradation Behavior. *Chem. Mater.* **2008**, *20*, 2655–2661.
29. Zucker, D.; Marcus, D.; Barenholz, Y.; Goldblum, A. Liposome Drugs' Loading Efficiency: A Working Model Based on Loading Conditions and Drug's Physicochemical Properties. *J. Controlled Release* **2009**, *139*, 73–80.
30. Goldbach, P.; Brochart, H.; Wehrlé, P.; Stamm, A. Sterile Filtration of Liposomes: Retention of Encapsulated Carboxyfluorescein. *Int. J. Pharm.* **1995**, *117*, 225–230.
31. Manconi, M.; Isola, R.; Falchi, A. M.; Sinico, C.; Fadda, A. M. Intracellular Distribution of Fluorescent Probes Delivered by Vesicles of Different Lipidic Composition. *Colloids Surf., B* **2007**, *57*, 143–151.

32. Ponce, A. M.; Vujaskovic, Z.; Fan, Y.; Needham, D.; Dewhirst, M. W. Hyperthermia Mediated Liposomal Drug Delivery. *Int. J. Hyperthermia* **2006**, *22*, 205–213.
33. Stamou, D.; Duschl, C.; Delamarche, E.; Vogel, H. Self-assembled microarrays of attoliter molecular vessels. *Angew. Chem. Int. Ed.* **2003**, *42*, 5580–5583.
34. Loew, M.; Kang, J.; Dähne, L.; Hendus-Altenburger, R.; Kaczmarek, O.; Liebscher, J.; Huster, D.; Ludwig, K.; Böttcher, C.; Herrmann, A.; Arbuzova, A. Controlled Assembly of Vesicle-Based Nanocontainers on Layer-by-Layer Particles *via* DNA Hybridization. *Small* **2009**, *5*, 320–323.
35. Lohse, B.; Bolinger, P.-Y.; Stamou, D. Encapsulation Efficiency Measured on Single Small Unilamellar Vesicles. *J. Am. Chem. Soc.* **2008**, *130*, 14372–14373.
36. Barbet, J.; Machy, P.; Truneh, A.; Leserman, L. D. Weak Acid-Induced Release of Liposome-Encapsulated Carboxyfluorescein. *Biochim. Biophys. Acta* **1984**, *772*, 347–356.
37. Hashizaki, K.; Taguchi, H.; Sakai, H.; Abe, M.; Saito, Y.; Ogawa, N. Carboxyfluorescein Leakage from Poly(ethylene glycol)-Grafted Liposomes Induced by the Interaction with Serum. *Chem. Pharm. Bull.* **2006**, *54*, 80–84.
38. Zelikin, A. N.; Quinn, J. F.; Caruso, F. Disulfide Cross-Linked Polymer Capsules: *En Route* to Biodeconstructible Systems. *Biomacromolecules* **2006**, *7*, 27–30.